Computerized Medical Imaging and Graphics 57 (2017) 10–18

Contents lists available at ScienceDirect

Computerized Medical Imaging and Graphics

journal homepage: www.elsevier.com/locate/compmedimag

Lung nodule classification using deep feature fusion in chest radiography

Changmiao Wang[a,b], Ahmed Elazab[a,b], Jianhuang Wu[a], Qingmao Hu[a,c,*]

[a] Shenzhen Institutes of Advanced Technology, Chinese Academy of Sciences, 1068 Xueyuan Boulevard, Shenzhen 518055, China
[b] University of Chinese Academy of Sciences, 52 Sanlihe Road, Beijing 100864, China
[c] Key Laboratory of Human-Machine Intelligence Synergy Systems, 1068 Xueyuan Boulevard, Shenzhen 518055, China

ARTICLE INFO

Article history:
Received 25 August 2016
Received in revised form 8 November 2016
Accepted 10 November 2016

Keywords:
Lung nodule
Computer aided diagnosis
Feature fusion
Deep learning

ABSTRACT

Lung nodules are small, round, or oval-shaped masses of tissue in the lung region. Early diagnosis and treatment of lung nodules can significantly improve the quality of patients' lives. Because of their small size and the interlaced nature of chest anatomy, detection of lung nodules using different medical imaging techniques becomes challenging. Recently, several methods for computer aided diagnosis (CAD) were proposed to improve the detection of lung nodules with good performances. However, the current methods are unable to achieve high sensitivity and high specificity. In this paper, we propose using deep feature fusion from the non-medical training and hand-crafted features to reduce the false positive results. Based on our experimentation of the public dataset, our results show that, the deep fusion feature can achieve promising results in terms of sensitivity and specificity (69.3% and 96.2%) at 1.19 false positive per image, which is better than the single hand-crafted features (62% and 95.4%) at 1.45 false positive per image. As it stands, fusion features that were used to classify our candidate nodules have resulted in a more promising outcome as compared to the single features from deep learning features and the hand-crafted features. This will improve the current CAD method based on the use of deep feature fusion to more effectively diagnose the presence of lung nodules.

1. Introduction

According to the World Cancer Report, lung cancer is the most common cause of cancer-related death in both men and women (Stewart and Wild, 2015). Overall, a lung cancer patient survives five years after diagnosis, and this rate is subject to increase to 49% in the early diagnosis (Schilham et al., 2006). Improving the chances of survival can be achieved by early detection of the lung nodules and enabling early treatment. As such, computer aided detection based on improved automated malignant nodule detection methods is a necessity. Computed tomography is considered to be a sensitive imaging modality for detecting lung cancer. However, chest radiology remains the most commonly used imaging modality for chest diseases as a balance of cost-effectiveness, dose-effectiveness, clinical availability, and ability to reveal unsuspected pathologic alterations (Garfinkel et al., 1995; Zhao et al., 2002). Over the years, computer aided diagnosis (CAD) systems have been demonstrated to be an effective assistant by observer performance studies (Kakeda et al., 2004; Kobayashi et al., 1996; MacMahon et al., 1999; Matsumoto et al., 1992), and feature computation is the key stage for these systems. The aim of these CAD systems is to aid radiologists in accurate nodule detection.

Anatomically, a lung nodule, which is typically less than 30 mm in diameter, is a small round growth of tissue that can be visualized by a chest X-ray. In general, we examine the posteroanterior views through the chest of the subject from back to front. The nodule can be either benign or malignant. However, as it becomes bigger, the possibility of malignancy increases. We note that computed tomography (CT) scans, which are based on single-line X-rays images extracted from various orientations, can provide a concise 3D view of the chest internals, which can more clearly detect shape, size, location, as well as density of the nodules. Therefore, the radiologists will be able to pick up the presence of nodules within the ribcage easily. However, what is needed is a reliable CAD technique that can automate the identification of lung nodules with high speed and accuracy. Nowadays, nodule detection algorithms can quickly identify these bright objects given the condition that they fulfill the requirements of having the expected size, shape, and

* Corresponding author at: Shenzhen Institutes of Advanced Technology, Chinese Academy of Sciences, 1068 Xueyuan Boulevard, Shenzhen 518055, China.
E-mail address: qm.hu@siat.ac.cn (Q. Hu).

http://dx.doi.org/10.1016/j.compmedimag.2016.11.004
0895-6111/

texture of a lung nodule in the suspected areas that are presented by chest X-ray.

For most systems, features like local features, shape features and spatial features, segmentation region and different positions within the lung are thought to be important for CAD systems. Nevertheless, these techniques used to derive good features is non-trival. Fortunately, deep neural networks have recently gained considerable interest for feature computation due to its ability to learn mid- and high-levels image representation. Rapid advances in deep neural networks have resulted in the development of new variants of convolutional neural networks (CNNs), which can be solved by efficient parallel processors in a graphics processing unit platform. We note that CNNs pertain to a feed-forward family of deep networks. In 2015, Shen et al. (Shen et al., 2015) investigated the lung nodule classification by multi-scale CNNs in CT screening. Moreover, since very large training sets are generally not available in the medical domain, Bar et al. explored the feasibility of using a deep learning approach based on non-medical learning in (Bar et al., 2015). Although high level features can be derived based on the transfer learning from classical deep learning model, they are not related to the medical image analysis task. The transferability of features decreases as the distance between the base task and the target task increases. However, transferring features from distant tasks can be better than using random features. This is the reason for the lower performance in medical image analysis task with high level features. Hence, in this paper, we explore the high level features from model based on transfer learning and fuse the hand-crafted features with deep features to classify the lung nodules in chest X-ray images. It is worthwhile noting that, deep learning methods have not been thoroughly tested for reducing false positive lung nodules, especially by utilizing non-medical archive learning. Our experiment results show that, the deep feature fusion may be sufficient in comparison with the hand-crafted features.

The rest of this paper is as follows. In Section 2, we introduce the preprocessing of the CAD system and the feature extraction by means of hand-crafted and deep model. We report the experimental results and discussion in Section 3. Finally, our conclusions are given in Section 4.

2. Material and methods

2.1. Public JSRT database

Our method is tested on a standard database that is acquired from the Japanese Society of Radiological Technology (JSRT), the detailed information is described in (Shiraishi et al., 2000). It contains 154 cases with confirmed lung nodules by CT and 93 normal cases without nodules. The images are digitized to 12-bit with 2048×2048 pixels at a resolution of 0.175 mm pixel size. The nodule size in diameter ranges from 5 to 40 mm. According to the degree of subtlety for detection, all the nodules are classified into five categories from obvious to extremely subtle. Only 140 nodules cases are chosen from the JSRT database because our CAD scheme is to detect nodules in the visible lung region. The characteristics of nodules are summarized in Tables 1 and 2, respectively.

2.2. Proposed method

Our nodule detection system consists of three modules. Fig. 1 shows the processing pipeline of our lung detection system. The first module aims to remove the ribs in chest radiographs. We adopted the rib suppression method based on principle component analysis (PCA) in order to improve the visibility of lung nodules (Ahmed et al., 2007; Hogeweg et al., 2010; Li et al., 2015). Next, the lung is segmented based on the customized active shape model (ASM) (Wu et al., 2015a), which allows us to obtain the general region of interest. The third module is to retrieve the candidate nodules by the generalized Laplacian of Gaussian (gLoG) method (Kong et al., 2013). Note that, we extract the features for the candidate nodules using hand-crafted and deep learning method in the final module to train the cost-sensitive random forest (CS-RF) to classify the lung nodule.

2.2.1. Preprocessing

Preprocessing is a preliminary stage in designing CAD systems. Its main goal is to enhance the characteristics of the image that could help to improve performance in following stages. Preprocessing includes removing the rib and segmentation of lung regions, which are detailed below.

2.2.1.1. Rib suppression. Some lung nodules cannot to be easily detected due to overlapping with the ribs or clavicles in the chest radiographs. Therefore, a rib suppression method is adopted to improve the visibility of lung nodules. There are mainly two types of methods to achieve rib suppression: learning based methods and statistical feature analysis based methods. The learning based methods need dual-energy radiographs as training data (Suzuki et al., 2004, 2005, 2006).

On the other hand, statistical feature analysis based methods are blind source analysis methods, and do not need dual-energy subtraction image as training sets. Such methods are based on independent component analysis (ICA) and PCA as in (Ahmed et al., 2007; Hogeweg et al., 2010; Rasheed et al., 2007). The PCA based methods achieve better suppression result than ICA methods. However, the rib segmentation is needed before PCA methods can be applied. The effectiveness of PCA based methods highly relies on the accuracy of rib segmentation. In this paper, we use the PCA method to remove rib. More information can be found in (Li et al., 2015). Fig. 2 shows an example of rib suppression on an image from JSRT database.

2.2.1.2. Lung field segmentation. The key step in CAD scheme for lung nodule detection in chest radiographs is the segmentation of the lung field. Many approaches have been proposed on segmentation of lung fields. These methods can be, broadly, classified into four categories: 1) rule-based techniques, 2) pixel classification techniques, 3) deformable model-based techniques, and 4) hybrid techniques. Although these methods yield the most accurate segmentation based on pixel classification, these methods result in non-desirable shapes. Hence, they need to be combined with ASM to account for the high variability of lung shapes. We use a customized ASM that includes initialization to separate the left and right lungs after finding the left and right boundaries of the trachea, and adopt a new objective function to impose distance and edge constraints on the ASM (Wu et al., 2015a). Fig. 3 shows an example of the final detected contours for the lung areas.

2.2.1.3. Nodule candidate detection. After preprocessing the image, the next step is to find any suspicious nodules. There are many methods for detecting the possible nodules, such as difference-image technique (Kakeda et al., 2004; Giger et al., 1988, 1990; Shih-Chung et al., 1993; Lo et al., 1995; Xu et al., 1997), convergence index (CI) filters (Hardie et al., 2008), and scale space representation method (Schilham et al., 2003, 2006; Lindeberg, 1998; Campadelli et al., 2006).

The scale space detection method was proposed by Ginneken et al. (Schilham et al., 2003, 2006) based on the scale space representation introduced by Lindeberg et al. (Lindeberg, 1998). The idea is to apply Laplacian of Gaussian (LoG) filter at several scales in order to highlight bright and roughly circular regions with different sizes. The conventional LoG kernels are rotational-symmetric while

Table 1
The number of lung nodules based on subtlety level and size.

Subtlety level	Small size (≤10 mm)	Medium size (>10 mm and ≤20 mm)	Large size (>20 mm)	Total
Extremely subtle	9	8	2	19(12.9%)
Very subtle	5	16	2	23(16.6%)
Subtle	10	29	9	48(34.6%)
Relatively obvious	5	26	7	38(27.3%)
Obvious	1	5	6	12(8.6%)
Total	30	84	26	140(100%)

Table 2
The number of lung nodule based on pathology and size.

Pathology	Small size (≤10 mm)	Medium size (>10 mm and ≤20 mm)	Large size (>20 mm)	Total
Benign	17	28	5	50(35.3%)
Malignant	13	56	21	90(64.7%)

the generalized Gaussian kernel, used in our method, has different scales and orientations which can be readily applicable to detect blobs with general elliptical shapes. That is to say, the gLoG filter cannot only accurately locate the blob centers, but also estimate the scales, shapes, and orientations of the detected blobs (Kong et al., 2013).

To achieve a trade-off between the number of detected nodules and the number of false positive, we use only scale from 0.5 to 3. By setting the appropriate parameter, we can get the 4570 candidate locations (on average 32.64 per image), and 87.9% (123/140) true nodules are detected. A candidate is labelled as a true nodule if it has the overlap with the "reference-standard" nodule area and the size of the candidate is nearly equal to the size of the "reference-standard" nodule area. After that, rule-based and the symmetry-based method are adopted to remove the false positives before proceeding to the next stage.

2.2.2. Feature extraction

Feature extraction is the key step in the CAD systems, such features have a major effect on their performance. Bram Van Ginneken et al. concluded most key features used in the CAD system (Van Ginneken et al., 2001). Kawata et al. computerized the topological and histogram feature spaces of the pulmonary nodules to classify the benign cases and malignant cases (Kawata et al., 2000). Wei et al. evaluated 210 features to look for the optimum feature set and gave the area under the receiver operating characteristic curve of the optimally selected feature set (Wei et al., 2002). Shiraishi et al. computed 71 features to detect the lung nodule (Shiraishi et al., 2006). Schiham et al. used a two-stage classifier with 10 and 20 features respectively (Schilham et al., 2006). Russell et al. segmented each nodule candidate and computed about 46 features for different classifiers to analysis the performance (Hardie et al., 2008). A supervised approach to discriminate between nodule and non-nodule segments by a set of representative image features was used by Ogul et al. (Oğul et al., 2015). However, inaccurate feature calculation and segmentation for complex objects can make new errors on its performance. It is difficult to get promising hand-crafted features which need professional prior knowledge on the designed task. Even though this is performed, we are still unable to achieve the most valuable feature for the task by hand-crafted feature engineering. These features can be divided into the following main groups: geometric features, intensity and contrast features, and features derived from first and second-order filters at different scales and directions. In this paper, we extract the hand-crafted features that are summarized in Table 3.

Recently, deep neural network has gained popularity because of its ability to learn mid- and high- levels image feature. The deep learning method was applied in many medical image analysis tasks where remarkable results could be achieved as in (Shen et al., 2015; Bar et al., 2015; Cireşan et al., 2013; Kim et al., 2013; Liao et al., 2013; Li et al., 2014a,b; Guo et al., 2015; Kumar et al., 2015; Lyndon et al., 2015a,b; Suk et al., 2015; Wu et al., 2015b). Deep learning methods are more powerful when applied on large training sets. However, the large datasets in the medical field are usually not available. Ideally, we can train a CNN by large number of medical datasets. However, we do not have enough medical data, and deep learning methods are most effective when applied to networks with large number of training data in order to train the deep neural network. We can attain the high level feature using deep learning method based on non-medical learning (Bar et al., 2015). Lately, many papers have been published in the general computer vision literature using transfer learning, which is an efficient way to utilize image representations learned with CNNs on large-scale annotated datasets. In particular, these are the target domains in which limited datasets exist.

In the computer vision domain, such large image sets exist (e.g. ImageNet) which enable the training of popular CNNs. In many image recognition tasks pertaining to the large scale visual recognition challenge of ImageNet, a few examples of such CNNs are Decaf, AlexNet, VGG, and Overfeat (Simonyan and Zisserman, 2014; Donahue et al., 2014; Sermanet et al., 2013; Krizhevsky et al., 2012). The CNNs were able to extract improved representations from raw data without requirement for domain knowledge. This was done with no hyper-parameter tuning, which suggested that further improvements could be made. This is important for the feature extraction as it can use CNNs or other deep learning strategies as a 'black box', whereby we will be able to achieve excellent machine learning performance neglecting the need of expert-designed feature extraction or domain knowledge.

The traditional studies primarily rely on lung nodule segmentation for regional analysis. We deal with the raw nodule patches by a hierarchical learning framework deep fusion features to extract discriminative features from, alternatingly, stacked layers. The AlexNet in (Krizhevsky et al., 2012) was trained over a subset of images from ImageNet containing 1000 categories and 1.2 million images. The network contains eight layers with weights: the first five are convolutional and the remaining three are fully-connected. For the fully-connected layers, each has 4096 neurons. The AlexNet won the first place in ImageNet classification in 2012. We extract the feature from the fully-connected layer on the pre-trained AlexNet model by the transfer learning to train our classifier.

However, some classical deep model feature did not achieve good results for a medical analysis task (Bar et al., 2015). Hence, we can fuse the deep feature obtained from the classical CNN model

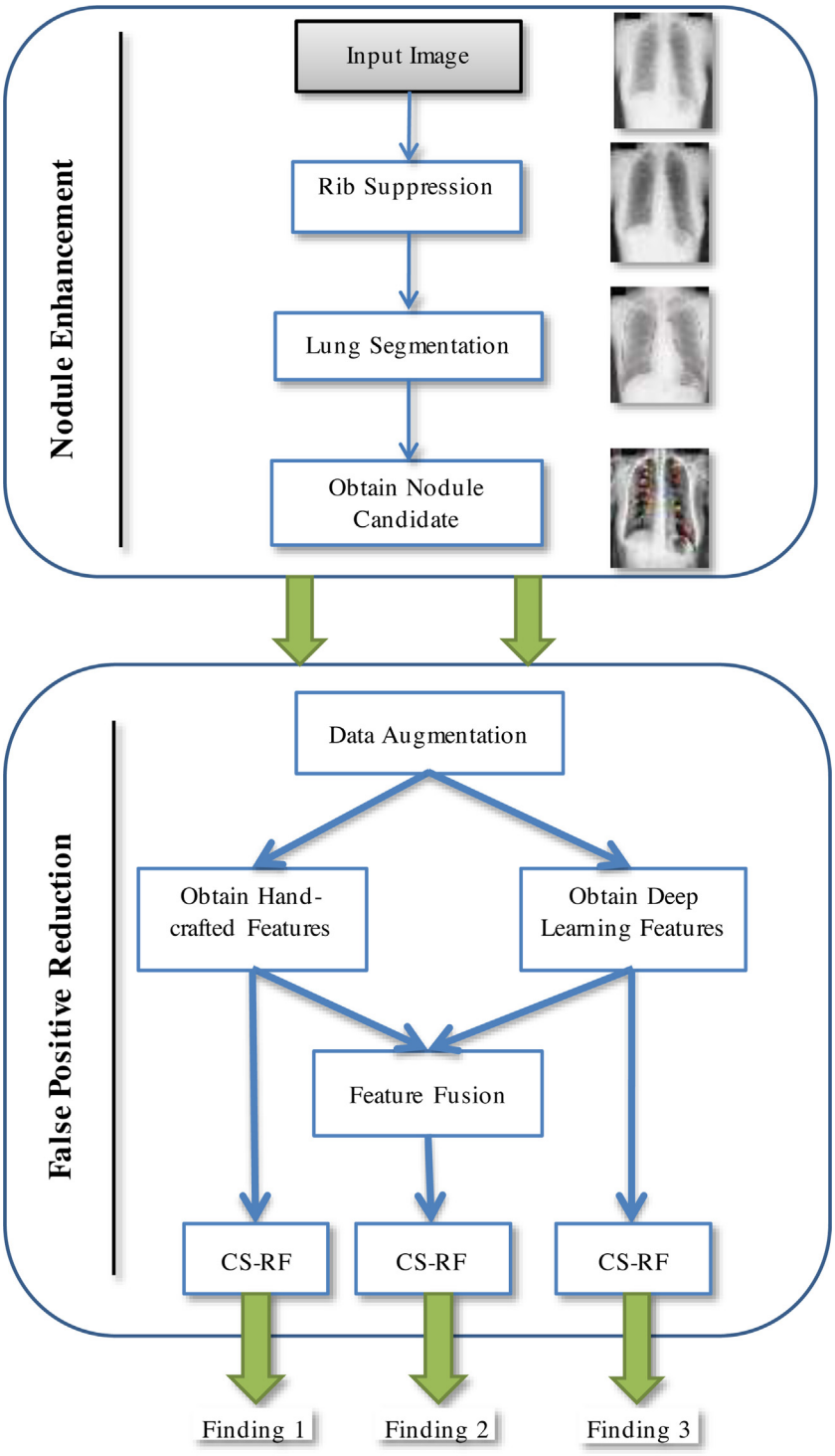

Fig. 1. Workflow diagram of the proposed method.

with the hand-crafted features for medical analysis task. We can use the cascade method to fuse the hand-crafted features with the deep features. After that, the PCA method is used to reduce the high cascade dimensions for the next stage. Finally, CS-RF is employed to reduce the false positive candidates.

The CAD system generates 4570 candidate locations (giving an average of 32.6 per image) among which 179 locations are true lung nodules. Note that 87.9% of all true nodules are among the candidates, demonstrating that, this is the maximally achievable sensitivity in this study. The class frequencies in the data are much imbalanced which will have a big impact on the performance of the CAD system. We carry out experiment to find that for a positive versus negative ratio being 1:20, the best sensitivity is only 0.493. As the positive samples are far less than the negative samples, we adopt data augmentation to increase the number of positive samples in the following way. The true lung nodule candidate position is translated with shift in 2, 4, 8 pixels, rotated with angle in 30°, 60°, 120°, 150°. Besides, we also use the RUSBoost method in (Seiffert

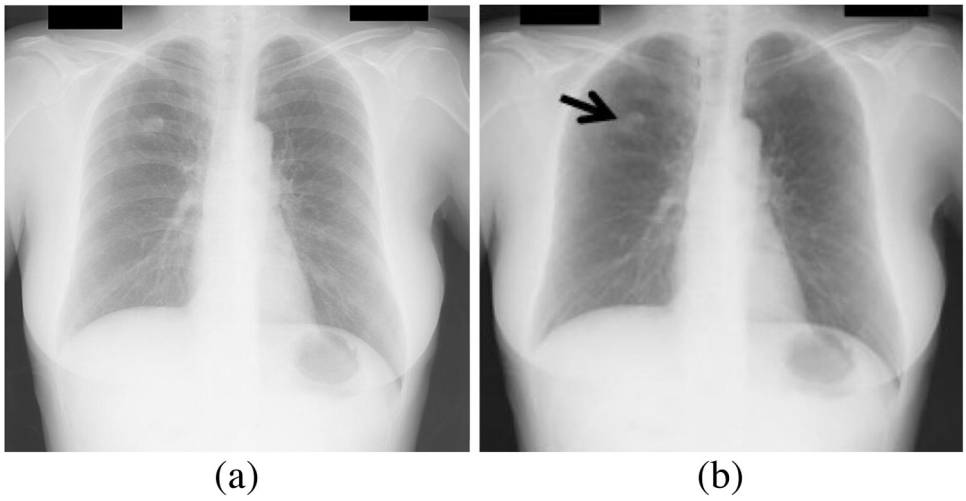

Fig. 2. The suppression and nodule detection result of chest X-ray images with tumor in JSRT database. The black arrow points to the location of lung nodule in the image. (a) The original image. (b) The rib suppressed image.

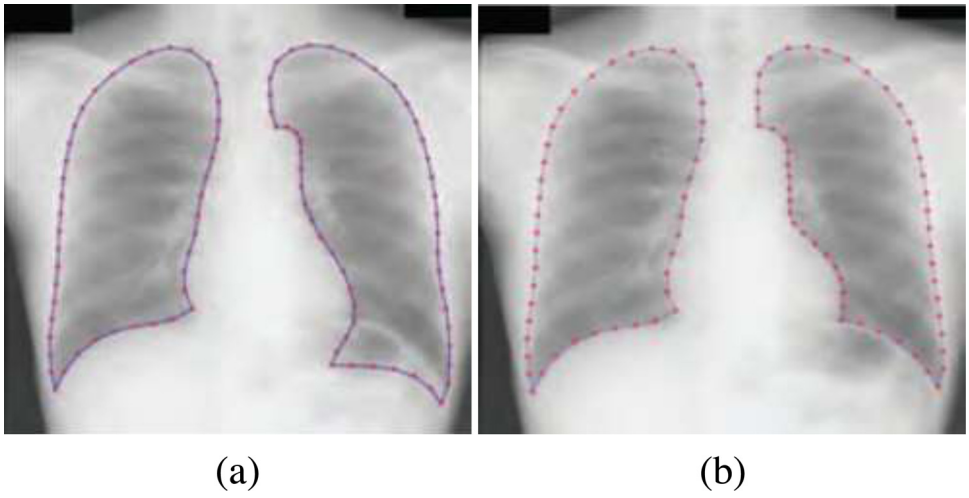

Fig. 3. Segmentation of one image from SCR database based on (a) the ASM without constraints, and (b) the employed ASM (Wu et al., 2015a).

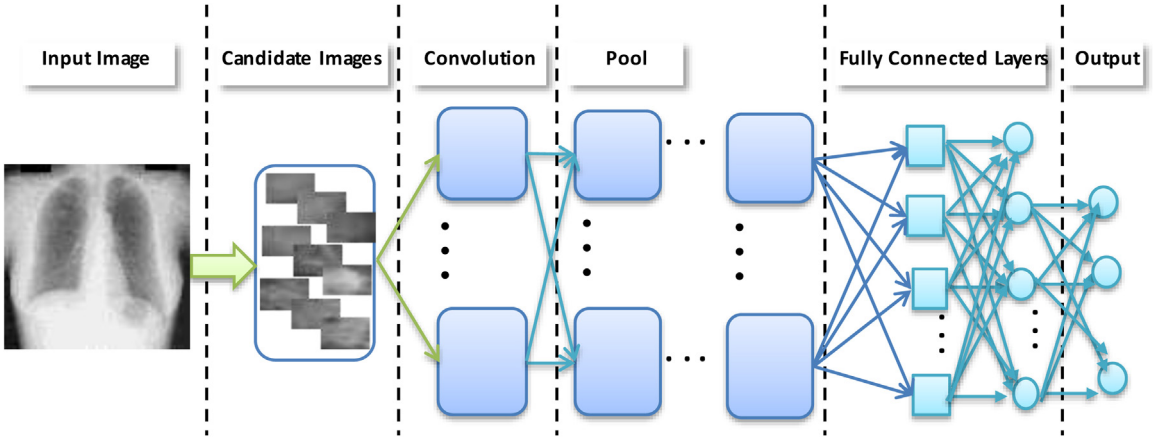

Fig. 4. The schematic design of the CNN of the AlexNet on the X-ray image adopted from (Krizhevsky et al., 2012).

Table 3
Hand-crafted features.

Geometric features of the candidate	Equivalent radius of the candidate region; Area; Circularity; Position and distance to pulmonary perimeter and hilum;
Intensity and Contrast features of the candidate	Maximum intensity inside the candidate region; Minimum intensity inside the candidate region; Mean intensity inside and standard deviation of the intensity distribution inside the candidate region; Maximum intensity along the boundary region; Minimum intensity along the boundary region; Mean intensity inside and standard deviation of the intensity distribution along the boundary region; Intensity skewness inside the candidate region; Intensity kurtosis insidethe candidate region; Intensity skewness along the boundary region; Intensity kurtosis along the boundary region; Energy inside the candidate region; Entropy inside the candidate region; Energy along the boundary region; Entropy along the boundary region; Central region – boundary contrast;
Features derived from first and second-order filters at different scales and directions	Gradient magnitude mean inside the candidate region; Gradient magnitude standard deviation inside the candidate region; Convergence coefficient mean inside the candidate region; Convergence coefficient standard deviation inside the candidate region; Blob strength (the norm of the gLoG filter); Radial-gradient mean inside the candidate region; Radial-gradient standard deviation inside the candidate region;

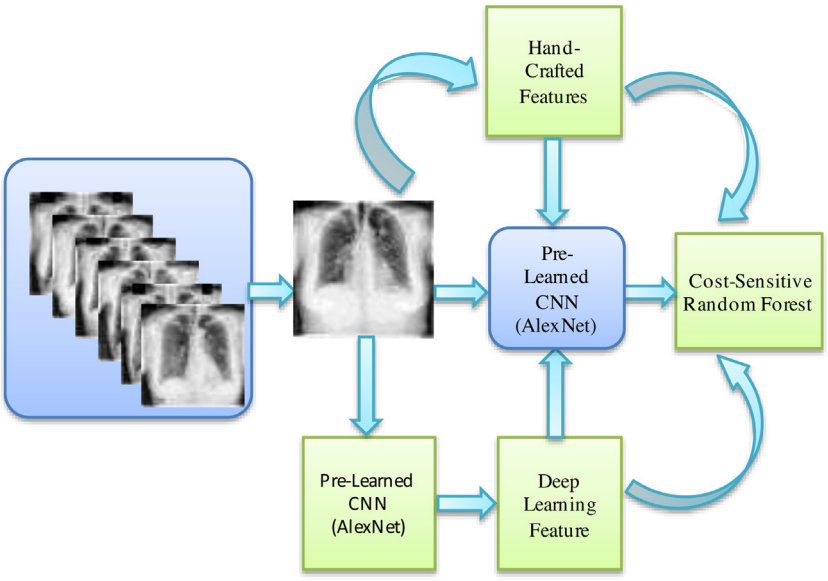

Fig. 5. Flowchart of feature extraction containing hand-crafted features and deep learning features to train the classifier.

et al., 2010) to increase the number of the positive samples. Through this data augmentation, the number of positive samples is increased from 179 to 4386, while the negative sample remains the same (4391). Finally, the CS-RF is learned to classify the lung nodule. The hand-crafted features include the intensity and contrast features, as well as the first and second-order filter features. For deep learning features, we use the features from the first fully connected layer of CNN as the input for a CS-RF classifier in cross-validation. The AlexNet model is trained over a subset of images from ImageNet of more than one million images that are categorized into 1000 categories, which is implemented in Caffe (Krizhevsky et al., 2012). Training the RF classifier is done using a 10-fold patch-based cross validation. Figs. 4 and 5 show the processing of extracting deep learning features.

We employ three commonly used metrics to quantitatively evaluate the performance of the proposed lung nodule detection method including sensitivity (*Sens*), specificity (*Spec*) and the average number of false positives per subject (*FP average*), which are defined as follows:

$$Sens = \frac{TP}{TP + FN},$$

$$Spec = \frac{TN}{TN + FP},$$

$$FP\ average = \frac{FP}{N},$$

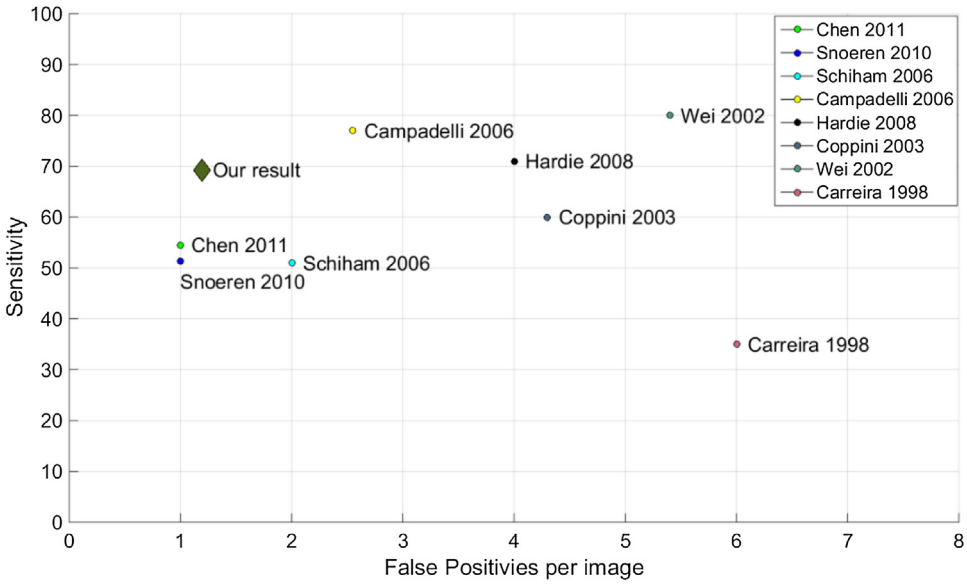

Fig. 6. Comparison of current published CAD systems based on the JSRT database.

where *TP*, *FP* and *FN* denote the total number of true-positive, false-positive and false-negative detection results, respectively, and *N* represents the number of subjects in the testing dataset.

For the candidate detection stage, the retrieval accuracy is vitally important, because we cannot find the true lung nodule that are missed by the lung nodule detection stage in the following discrimination stage. We only consider the visual lung region and the criterion of true lung nodule is determined by the distance between the centroid of detection region and the ground truth. Our method can achieve a good balance between retrieval accuracy and the false positive candidates.

In our experiments, the rule-based and symmetry method are used for reducing the false positive without losing the true lung nodule after we get the preliminary candidate lung nodule. Only a small number of candidates is obtained, which dramatically reduces the computational workload in the following stage. By employing the candidate lung nodule sample from the training set, we can train the CS-RF in order to remove the false positive candidates and accurately identify the true lung nodules.

We employ common feature extraction procedure on our dataset and utilize a CS-RF classifier for our prediction. For the hand-crafted features, we extract intensity-based, geometry-based, and multiple order filter features (Table 3). For the deep learning feature, we extract the deep feature by transfer learning on the candidate regions. The flowchart of the feature extraction is shown in the Fig. 5.

3. Results and discussion

We extracted the hand-crafted features and deep learning features, as well as developed integrated features characteristics, and made use of these features to perform machine learning which yield the results in Table 4.

We compare the performance of our method with single hand-crafted features and single deep learning features. For the test, we use 10-fold cross-validation by randomly separating the images into ten equally sized sets. The final test result is the average of ten iterations, in which every iteration we use the candidates from the nine sets for training and the left set for testing. The results are shown in Fig. 6 and summarized in Table 4, respectively. The results

Table 4
Comparison results of the performance of our method with single hand-crafted features and single deep learning features.

Feature	10-fold
Hand-crafted Feature	*Sens*: 0.620 *Spec: 0.954* *FP: 1.45*
Deep Learning Feature	*Sens*: 0.659 *Spec: 0.959* *FP: 1.3*
Fusion Feature	*Sens*: 0.693 *Spec: 0.962* *FP: 1.19*

show that, the fusion feature may be sufficient to classify the lung nodule.

Preprocessing has a big impact on the performance of our method. On one hand, the best achieved sensitivity/specificity is 0.493/0.952 without augmentation to have a ratio of positive samples to negative samples being 1:20. After data augmentation, the best sensitivity/specificity is 0.693/0.962. On the other hand, we carry out comparative experiments to illustrate the impact of rib suppression. The number of candidate locations is 4928 without rib suppression, which is decreased to 4570 with rib suppression. The sensitivity and specificity are, respectively, 0.693/0.962 at 1.19 false positive per image and 0.649/0.984 at 2.25 false positive per image with/without rib suppression. Thus rib suppression increases the specificity (from 0.962 to 0.984) at the expense of decreased sensitivity (from 0.693 to 0.649).

Many methods have been proposed to test the JSRT database in (Schilham et al., 2006; Hardie et al., 2008; Campadelli et al., 2006; Wei et al., 2002; Carreira et al., 1998; Coppini et al., 2003; Snoeren et al., 2010; Chen et al., 2011). The comparative results are shown in Fig. 6. Compared with Chen et al. (Chen et al., 2011), our method yields higher (0.692 versus 0.510) and a poorer FP (1.19 versus 1.00). The better FP of Chen et al. (Chen et al. 2011) may be due to the confinement of lung nodule candidate through segmentation, while our method uses square patch followed by extracting the features from the CNNs by transfer learning which could yield more candidates. The sensitivity is higher due to the rib suppression and the feature fusion method we use. For other methods listed

in Fig. 6, they have a false positive bigger than 2, which will be hard to be used clinically. For the commercial software by Riverain (Kligerman et al., 2013; Schalekamp et al., 2014), as it uses additional data in addition to JSRT data, it is understandable that it yields better performance (sensitivity = 75%, and false positive = 0.5).

Here is a summarization of our contribution. We derive a new characteristic feature that is able to yield lower false positive and a higher sensitivity. Besides, we are able to obtain features that are based on CNN model learning from the non-medical data especially for medical data which lacks ground truth. We combine hand-crafted features with learned features and reduce the feature dimension through PCA.

In the future we are going to enhance the performance through direct learning via huge medical database or fine tuning existing CNNs.

4. Conclusion

In this paper, we demonstrated the effectiveness of deep feature fusion for the classification the lung nodules. Without using very large training sets for learning the deep model in lung nodule domain, we explored the feasibility of using a deep learning approach based on non-medical learning deep model. Independent feature from the existing deep learning model might cause a lower performance compared with the hand-crafted features for classification as the deep model captures other information with less relation to the classification of the lung nodule. However, the deep feature fusion from the deep model and hand-crafted features could outperform the single hand-crafted features. Feature fusion was used to classify the candidate nodules and resulted in a more promising outcome compared with the single feature from deep learning features and the hand-crafted features. For further improvement of our method, we plan to remove the clavicle and build big dataset for training intermediary deep network from clinical data in our future work.

Acknowledgments

This work has been supported by: National Program on Key Basic Research Project (Nos. 2013CB733800, 2012CB733803), Key Joint Program of National Natural Science Foundation and Guangdong Province (No. U1201257), Shenzhen Key Basic Research Program (No. JCYJ20160331191401141), and National Natural Science Foundation of China (No. 61671440).

References

Ahmed, B., Rasheed, T., Khan, M.A., Cho, S.J., Lee, S., Kim, T.-S., 2007. Rib suppression for enhancing frontal chest radiographs using independent component analysis Adaptive and Natural Computing Algorithms. In: International Conference on Adaptive and Natural Computing Algorithms. Springer, Berlin Heidelberg, pp. pp. 300–308.

Bar, Y., Diamant, I., Wolf, L., Greenspan, H., 2015. Deep learning with non-medical training used for chest pathology identification. SPIE Medical Imaging. International Society for Optics and Photonics 94140V, 94140V–941407.

Campadelli, P., Casiraghi, E., Artioli, D., 2006. A fully automated method for lung nodule detection from postero-anterior chest radiographs. IEEE Trans. Med. Imaging. 25 (12), 1588–1603.

Carreira, M.a.J., Cabello, D., Penedo, M.G., Mosquera, A., 1998. Computer-aided diagnoses: automatic detection of lung nodules. Med. Phys. 25 (10), 1998–2006.

Chen, S., Suzuki, K., MacMahon, H., 2011. Development and evaluation of a computer-aided diagnostic scheme for lung nodule detection in chest radiographs by means of two-stage nodule enhancement with support vector classification. Med. Phys. 38 (4), 1844–1858.

Cireşan, D.C., Giusti, A., Gambardella, L.M., Schmidhuber, J., 2013. Mitosis detection in breast cancer histology images with deep neural networks. In: International Conference on Medical Image Computing and Computer-assisted Intervention 2013. Springer, pp. 411–418.

Coppini, G., Diciotti, S., Falchini, M., Villari, N., Valli, G., 2003. Neural networks for computer-aided diagnosis: detection of lung nodules in chest radiograms. IEEE Trans. Inf. Technol. Biomed. 7 (4), 344–357.

Donahue, J., Jia, Y., Vinyals, O., Hoffman, J., Zhang, N., Tzeng, E., Darrell, T., 2014. DeCAF: a deep convolutional activation feature for generic visual recognition. In: International Conference on Machine Learning., pp. 647–655.

Garfinkel, L., Murphy, G., Lawrence, W.J., Lenhard, R.J., 1995. American Cancer Society Textbook of Clinical Oncology. The Society Press.

Giger, M.L., Doi, K., MacMahon, H., 1988. Image feature analysis and computer-aided diagnosis in digital radiography. 3. Automated detection of nodules in peripheral lung fields. Med. Phys. 15 (2), 158–166.

Giger, M.L., Ahn, N., Doi, K., MacMahon, H., Metz, C.E., 1990. Computerized detection of pulmonary nodules in digital chest images: use of morphological filters in reducing false-positive detections. Med. Phys. 17 (5), 861–865.

Guo, Y., Gao, Y., Shen, D., 2015. Deformable MR prostate segmentation via deep feature learning and sparse patch matching. IEEE Trans. Med. Imaging 35 (4), 1077–1089.

Hardie, R.C., Rogers, S.K., Wilson, T., Rogers, A., 2008. Performance analysis of a new computer aided detection system for identifying lung nodules on chest radiographs. Med. Image Anal. 12 (3), 240–258.

Hogeweg, L.E., Mol, C., de Jong, P.A., van Ginneken, B., 2010. Rib suppression in chest radiographs to improve classification of textural abnormalities. SPIE Med. Imaging, pp. 76240Y–762406.

Kakeda, S., Moriya, J., Sato, H., Aoki, T., Watanabe, H., Nakata, H., Oda, N., Katsuragawa, S., Yamamoto, K., Doi, K., 2004. Improved detection of lung nodules on chest radiographs using a commercial computer-aided diagnosis system. Am. J. Roentgenol. 182 (2), 505–510.

Kawata, Y., Niki, N., Ohmatsu, H., Kusumoto, M., Kakinuma, R., Mori, K., Nishiyama, H., Eguchi, K., Kaneko, M., Moriyama, N., 2000. Computerized analysis of pulmonary nodules in topological and histogram feature spaces. In: 15th International Conference on Pattern Recognition., pp. 332–335.

Kim, M., Wu, G., Shen, D., 2013. Unsupervised deep learning for hippocampus segmentation in 7.0 tesla MR images. In: Machine Learning in Medical Imaging. Springer, pp. 1–8.

Kligerman, S., Cai, L., White, C.S., 2013. The effect of computer-aided detection on radiologist performance in the detection of lung cancers previously missed on a chest radiograph. J. Thorac. Imaging 28 (4), 244–252.

Kobayashi, T., Xu, X.-W., MacMahon, H., Metz, C.E., Doi, K., 1996. Effect of a computer-aided diagnosis scheme on radiologists' performance in detection of lung nodules on radiographs. Radiology 199 (3), 843–848.

Kong, H., Akakin, H.C., Sarma, S.E., 2013. A generalized Laplacian of Gaussian filter for blob detection and its applications. IEEE Trans. Cyber. 43 (6), 1719–1733.

Krizhevsky, A., Sutskever, I., Hinton, G.E., 2012. Imagenet classification with deep convolutional neural networks. Advances in Neural Information Processing Systems, 1097–1105.

Kumar, D., Wong, A., Clausi, D.A., 2015. Lung nodule classification using deep features in CT images. In: 12th IEEE Conference on Computer and Robot Vision (CRV). pp. 133–138.

Li, F., Tran, L., Thung, K.-H., Ji, S., Shen, D., Li, J., 2014a. Robust deep learning for improved classification of AD/MCI patients. In: In: International Workshop on Machine Learning in Medical Imaging. Springer, pp. 40–247.

Li, R., Zhang, W., Suk, H.-I., Wang, L., Li, J., Shen, D., Ji, S., 2014b. Deep learning based imaging data completion for improved brain disease diagnosis. In: Medical Image Computing and Computer-Assisted Intervention–MICCAI 2014. Springer, pp. 305–312.

Li, X., Luo, S., Hu, Q., Li, J., Wang, D., 2015. Rib suppression in chest radiographs for lung nodule enhancement. In: IEEE International Conference on Information and Automation.

Liao, S., Gao, Y., Oto, A., Shen, D., 2013. Representation learning: a unified deep learning framework for automatic prostate MR segmentation. In: Medical Image Computing and Computer-Assisted Intervention–MICCAI 2013. Springer, pp. 254–261.

Lindeberg, T., 1998. Feature detection with automatic scale selection. Int. J. Comput. Vision 30 (2), 79–116.

Lo, S.-C.B., Lou, S.-L.A., Lin, J.-S., Freedman, M.T., Chien, M.V., Mun, S.K., 1995. Artificial convolution neural network techniques and applications for lung nodule detection. IEEE Trans. Med. Imaging 14 (4), 711–718.

Lyndon, D., Kumar, A., Kim, J., Leong, P.H., Feng, D., 2015a. Convolutional neural networks for subfigure classification. Working Notes CLEF, 2015.

Lyndon, D., Kumar, A., Kim, J., Leong, P.H., Feng, D., 2015b. Convolutional Neural Networks for Medical Clustering. CLEF.

MacMahon, H., Engelmann, R., Behlen, F.M., Hoffmann, K.R., Ishida, T., Roe, C., Metz, C.E., Doi, K., 1999. Computer-aided diagnosis of pulmonary nodules: results of a large-Scale observer test. Radiology 213 (3), 723–726.

Matsumoto, T., Yoshimura, H., Giger, M.L., Doi, K., Macmahon, H., Montner, S.M., Nakanishi, T., 1992. Potential usefulness of computerized nodule detection in screening programs for lung cancer. Invest. Radiol. 27 (6), 471–475.

Oğul, B.B., Koşucu, P., Özçam, A., Kanik, S.D., 2015. Lung nodule detection in X-Ray images: a new feature set. In: 6th European Conference of the International Federation for Medical and Biological Engineering. Springer, pp. 150–155.

Rasheed, T., Ahmed, B., Khan, M.A., Bettayeb, M., Lee, S., Kim, T.-S., 2007. Rib suppression in frontal chest radiographs: a blind source separation approach. 9th International Symposium on Signal Processing and Its Applications, 1–4.

Schalekamp, S., van Ginneken, B., Karssemeijer, N., Schaefer-Prokop, C., 2014. Chest radiography: new technological developments and their applications. In: Seminars in respiratory and critical care medicine, pp. 003–016.

Schilham, A.M., van Ginneken, B., Loog, M., 2003. Multi-scale nodule detection in chest radiographs. In: Medical Image Computing and Computer-Assisted Intervention-MICCAI 2003. Springer, pp. 602–609.
Schilham, A.M., Van Ginneken, B., Loog, M., 2006. A computer-aided diagnosis system for detection of lung nodules in chest radiographs with an evaluation on a public database. Med. Image Anal. 10 (2), 247–258.
Sermanet, P., Eigen, D., Zhang, X., Mathieu, M., Fergus, R., LeCun, Y., 2013. Overfeat: Integrated recognition, localization and detection using convolutional networks. arXiv preprint ArXiv:1312.6229.
Seiffert, C., Khoshgoftaar, J., Van Hulse, A., 2010. RUSBoost: A hybrid approach to alleviating class imbalance. IEEE Transactions Systems, Man, and Cybernetics Part A: Systems and Humans 40 (1), 185–197.
Shen, W., Zhou, M., Yang, F., Yang, C., Tian, J., 2015. Multi-scale convolutional neural networks for lung nodule classification. In: Information Processing in Medical Imaging. Springer, pp. 588–599.
Shih-Chung, B.L., Freedman, M.T., Lin, J.-S., Mun, S.K., 1993. Automatic lung nodule detection using profile matching and back-propagation neural network techniques. J. Digit. Imaging 6 (1), 48–54.
Shiraishi, J., Katsuragawa, S., Ikezoe, J., Matsumoto, T., Kobayashi, T., Komatsu, K.-i., Matsui, M., Fujita, H., Kodera, Y., Doi, K., 2000. Development of a digital image database for chest radiographs with and without a lung nodule: receiver operating characteristic analysis of radiologists' detection of pulmonary nodules. Am. J. Roentgenol. 174 (1), 71–74.
Shiraishi, J., Li, Q., Suzuki, K., Engelmann, R., Doi, K., 2006. Computer-aided diagnostic scheme for the detection of lung nodules on chest radiographs: localized search method based on anatomical classification. Med. Phys. 33 (7), 2642–2653.
Simonyan, K., Zisserman, A., 2014. Very deep convolutional networks for large-scale image recognition arXiv preprint arXiv:1409.1556.
Snoeren, P.R., Litjens, G.J., Ginneken, B., Karssemeijer, N., 2010. Training a computer aided detection system with simulated lung nodules in chest radiographs. In: The Third International Workshop on Pulmonary Image Analysis. pp. 139–149.
Stewart, B., Wild, C.P., 2015. World Cancer Report 2014. WHO Press.
Suk, H.-I., Lee, S.-W., Shen, D., A.S.D.N, 2015. Initiative, Deep sparse multi-task learning for feature selection in Alzheimer's disease diagnosis. Brain Struct. Funct., 1–19.
Suzuki, K., Abe, H., Li, F., Doi, K., 2004. Suppression of the contrast of ribs in chest radiographs by means of massive training artificial neural network. In: International Society for Optics and Photonics on Medical Imaging 2004., pp. 1109–1119.
Suzuki, K., Shiraishi, J., Li, F., Abe, H., MacMahon, H., Doi, K., 2005. Effect of massive training artificial neural networks for rib suppression on reduction of false positives in computerized detection of nodules on chest radiographs. In: International Society for Optics and Photonics on Medical Imaging 2005, 97–103.
Suzuki, K., Abe, H., MacMahon, H., Doi, K., 2006. Image-processing technique for suppressing ribs in chest radiographs by means of massive training artificial neural network (MTANN). IEEE Trans. Med. Imaging 25 (4), 406–416.
Van Ginneken, B., ter Haar Romeny, B.M., Viergever, M.A., 2001. Computer-aided diagnosis in chest radiography: a survey. IEEE Trans. Med. Imaging 20 (12), 1228–1241.
Wei, J., Hagihara, Y., Shimizu, A., Kobatake, H., 2002. Optimal image feature set for detecting lung nodules on chest X-ray images. In: CARS 2002 Computer Assisted Radiology and Surgery. Springer, pp. 706–711.
Wu, G., Zhang, X., Luo, S., Hu, Q., 2015a. Lung segmentation based on customized active shape model from digital radiography chest images. J. Med. Imaging Health Inf. 5 (2), 184–191.
Wu, G., Kim, M.-J., Wang, Q., Munsell, B., Shen, D., 2015b. Scalable high performance image registration framework by unsupervised deep feature representations learning. IEEE Trans. Biomed. Eng. 63 (7), 1505–1516.
Xu, X.-W., Doi, K., Kobayashi, T., MacMahon, H., Giger, M.L., 1997. Development of an improved CAD scheme for automated detection of lung nodules in digital chest images. Med. Phys. 24 (9), 1395–1403.
Zhao, H., Lo, S.-C.B., Freedman, M.T., Wang, Y.J., 2002. Enhanced lung cancer detection in temporal subtraction chest radiography using directional edge filtering techniques. International Society for Optics and Photonics on Medical Imaging, pp. 698–703.